Journal of Applied Electrochemistry **31**: 845–853, 2001.

Electrochemical supercapacitors based on industrial carbon blacks in aqueous H_2SO_4

F. BECK[1], M. DOLATA[1], E. GRIVEI[2] and N. PROBST[2]
[1]*Universität Duisburg, Fachgebiet Elektrochemie, D-47057 Duisburg, Germany*
[2]*ERACHEM Europe, B-2830 Willebroek, Belgium*

Received 10 February 2000; accepted in revised form 7 January 2001

Key words: carbon black (CB), constant current cycling (CCC), electrochemical super capacitor (ECSC), model cell, pseudo capacitance

Abstract

It is shown that industrial carbon blacks (CBs) are interesting materials for electrochemical supercapacitors (ECSCs). The specific areas A_s ranged from 28 to 1690 $m^2\ g^{-1}$. The highest values were realized through activation in CO_2 at 1100 °C. Precompacted carbon black electrodes with 5–10 wt % PTFE as a binder in the pellet in 10–12 M H_2SO_4 were characterized by constant current cycling, CCC, j = 20–50 mA cm^{-2}. Voltage–time curves showed nearly pure capacitive behaviour. Specific capacitance of single electrodes, $C_{s,1}$, could be derived therefrom. A plot of $C_{s,1}$ against A_s shows a linear behavior according to $C_{s,1} = C_{A,DL}A_s$, where $C_{A,DL}$ is the Helmholtz double layer capacitance per atomic surface area. Best fit was obtained with $C_{A,DL}$ = 16 μF cm^{-2}. The highest experimental values, $C_{s,1}$ = 250 F g^{-1}, are due to 60% of the theoretical maximum, which corresponds to an A_s calculated from both faces of isolated graphene layers. Only marginal pseudocapacitances are observed. *Model cells* for ECSCs (with microporous Celgard™ separators) could be extensively cycled (CCC). A monopolar cell endured $Z > 2000$ cycles. Bipolar cells (5 units) allowed 700 cycles. Practical problems such as the development of electrode holders and of carbon black filled polypropylene composites for current collectors are discussed. It is concluded that entirely metal-free ECSCs with low cost can be produced.

1. Introduction

Highly dispersed or porous carbons are known as versatile materials for electrochemical supercapacitors (ECSCs). An essential feature is the absolute corrosion stability in nonoxidizing aqueous electrolytes, even in strong acids. Beck and Krüger [1, 2] have introduced carbon blacks (CBs) from various industrial sources for this application. CBs are produced on a large scale, predominantly as fillers for tyres [3]. 95% is due to the furnace process. In general there are many properties of carbon and graphite to be of high interest in electrochemistry [4]. Activated carbons (ACs) have been employed since 1980 as another material, the first ECSCs were manufactured on this basis [5, 6] and have been preferred by most other workers [7–9]. Sometimes carbon fibers are recommended [10]. More sophisticated materials such as C-aerogels have also been proposed [11]. A combination with a graphite positive led to the metal-free all-carbon accumulator [12, 13]. Aqueous H_2SO_4 is selected as electrolyte to achieve a high conductivity [1, 2, 5–7, 9–13]. KOH is also used [8, 14] in spite of the strong nucleophilic character of the OH^--ions. Nonaqueous electrolytes, on the other hand, allow a wider choice of current collector material, which may be even made from Al [15], cf. paragraph 3.5. A common feature of all these developments is a high specific area of the C-material [16].

We report here on a further exploitation of the CB basis. The paper deals with the electrochemical characterization at laboratory scale. Typical areas of the single cylindrical pellet-electrodes, both sided, were 4.54 cm^2. The cylindrical horizontal cells consisting of a pair of such electrodes had an area of 7.0 cm^2.

2. Experimental details

Table 1 lists 24 *industrial carbon blacks* which were employed in the course of this work. They are characterized by the specific area A_s (BET). A_s covers a wide range from 28 to 1690 $m^2\ g^{-1}$. The primary particle diameters are relatively uniform, about 20 nm. Two groups must be distinguished:

(I) Former samples [1, 2] from five manufacturers (e.g., Cabot, Columbia and Degussa).
(II) More recent samples 'ENSACO ... MM GRAN' from ERACHEM Europe, the former MMM Carbon Comp.

The dashed line in Table 1 divides the CBs into two other groups, associated with nanoporosity. This will be discussed in Section 3.3. The highest BET values were

Table 1. Industrial carbon blacks: powders and pearls

Type	Manufacturer	Material	BET surface $A_s/m^2\,g^{-1}$
Raven 410*	Columbia	Powder	28
ENSACO 150 MM GRAN	MMM Carbon	Powder	47
ENSACO 26 MM GRAN	MMM Carbon	Powder	61
Printex 150 T	Degussa	Powder	110
Corax L (Printex L)	Degussa	Powder	150
ENSACO 8 MM GRAN	MMM Carbon	Powder	213
Vulcan XC 72	Cabot	Powder	254
Corax (Printex) L6	Degussa	Powder	265
FW 200$^+$	Degussa	Powder	460
Monarch 1300	Cabot	Powder	560
Black Pearls 1300	Cabot	Pearls	560
ENSACO 23 MM GRAN	MMM Carbon	Powder	640
Darco S 51 RL	Atlas	Powder	650
ENSACO 350 GRAN	MMM Carbon	Powder	804
Ketjen Black	AKZO	Powder	950
ENSACO 51 MM GRAN	MMM Carbon	Powder	1000
Printex XE2	Degussa	Pearls	1000
Conductex 40-220	Columbia	Powder	1075
ENSACO 52 MM	MMM Carbon	Powder	1100
ENSACO 61 MM	MMM Carbon	Powder	1300
ES 06 MM	MMM Carbon	Powder	1300
ENSACO 56 MM	MMM Carbon	Powder	1350
Black Pearls 2000	Cabot	Pearls	1475
ENSACO 114 MM	MMM Carbon	Powder	1690

Primary particle diameter, $2r = 13$–30 nm.
* Black pigment.
$^+$ O-surface groups.

obtained by 'etching' the CB particles through the Boudouard reaction at about 750–1100 °C:

$$C + CO_2 \longrightarrow 2\ CO \qquad (1)$$

Unfortunately, the losses due to a gasification of carbon through Equation 1 increased with increasing BET surfaces.

The nonstirred 'electrolyte' was 10 M or 12 M H_2SO_4. It was analytical grade. These concentrations are fully compatible to both of the eventual limitations:

(i) The CB electrodes have an average porosity of about 70 vol % [1, 2]. The pellet electrodes are immediately wetted on immersion. The amount of electrolyte which can be stored in the pores is in excess with respect to the need for counterions at the surface.
(ii) The all-C accumulator C/graphite must be cycled in this concentration range. At $c < 10$ M the GIC-positive becomes irreversible due to the formation of graphite oxide. At $c > 12$ M a cathodic reduction of H_2SO_4 becomes possible [17] to form S, SO_2 and H_2S.

The electrolyte is in large excess in the case of the single electrode measurements.

The CB-material (powders) was further processed to a precompacted CB electrode, PCCBE (cylindrical pellet) in two steps: (i) Binder: Admixture of $c_B = 2$–10 wt % (in most cases 5–10 wt %) PTFE (as 60% dispersion in water, drying step) to the CB; and (ii) Compaction in a steel mould at $p_{PC} \geq 10$ MPa (100 bar). Our standard was 440 MPa for pellet electrodes. As shown in [1], p_{PC} can be even lowered to 0.1 MPa (1 bar).

Practically no relaxation in V and ρ was found after removing the external pressure. ρ fell from about 1 Ω cm to 0.05 Ω cm on precompaction, which is the order of glassy carbon [18].

Electrode holders for this kind of working electrode are described in [1, 2] as a wet contact with a Pt/Ir mesh (enveloping design). An amended version is shown in [19], where two Ti frames with two loosely contacted Pt/Ir meshes are attached by PP-screws. These holders are very useful for the polarization in the positive direction. However, for a polarization in the negative direction, Pt is inappropriate due to it's small hydrogen overvoltage. An electrode holder shown in Figure 1 was developed. The contact material was graphite foil, Grafoil^{TM} from UCC or Sigraflex^{TM} from Sigri, which has a medium hydrogen overvoltage.

Further problems associated with the single electrode will be discussed in Section 3.1.

The counter electrode was a small Pt sheet. The reference electrode was a $Hg/Hg_2SO_4/1$ M H_2SO_4 electrode, which has a potential of 674 mV vs SHE. The potentials are denoted as U_S. The electrolytes were purged with Ar and the temperature was 20 °C.

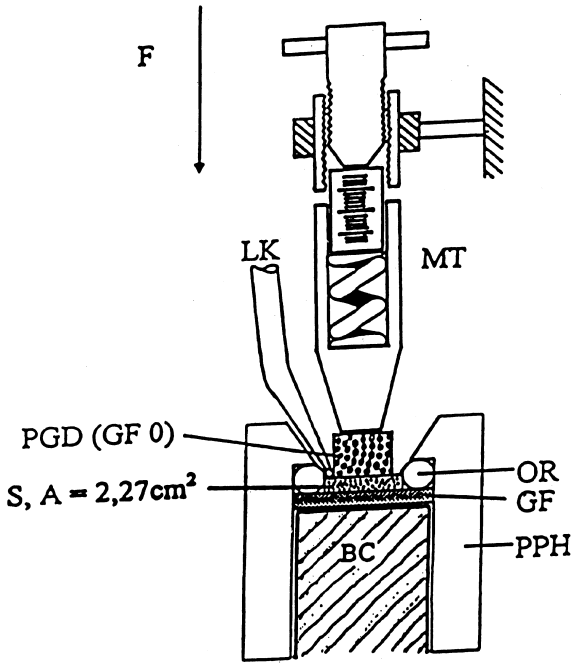

Fig. 1. Working electrode for negative potentials. Key: (LK) Luggin capillary; (S) sample; (PGD) porous sintered glass disc; (PPH) polypropylene holder; (GF) Grafoil^{RTM} sheet; (OR) O-ring; (BC) brass contact and (MT) mechanical tool for pressurizing.

3. Results and discussions

3.1. *Electrode design*

PTFE (dispersion) was employed as a standard binder. The concentration c_B in the PCCB electrode was varied between 1 and 10%. Figure 2 shows the dependency of the specific capacitance of single electrodes, $C_{s,1}$, on c_B. Interestingly, some loss (−10%) in $C_{s,1}$ was found for low binder concentrations $c_B = 1$ and 2%, and it was only for $c_B = 5$ and 10% that the maximum was obtained. The density of this PCCB electrode was 0.5–0.7 g cm^{-3}, as was the case for the other CBs. But there was one exception. CB E 52 had a density of 1.3 g cm^{-3}.

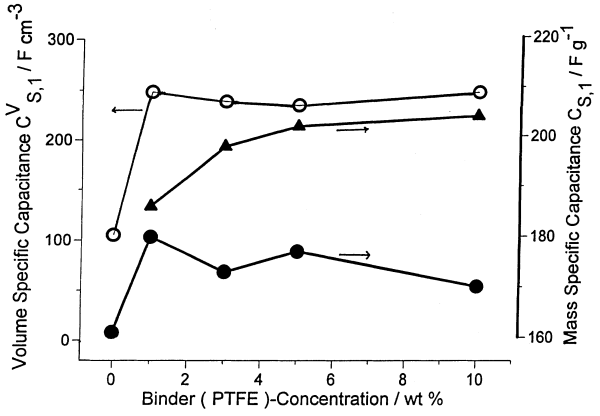

Fig. 2. Dependency of mass and volume-specific capacitances of single electrodes, $C_{s,1}$ and $C^v_{s,1}$ on the concentration of the PTFE binder. Key: (●, ○) CB: ENSACO 52 MM, and (▲) CB: ENSACO 61 MM.

But the yield in the furnace process was only 1%. 99% of the CB burnt away in this case. Figure 2 shows that $C_{s,1}$ was constant down to 1% PTFE. The volume specific capacitance, $C^v_{s,1}$, was accordingly high.

Resistivity ρ was about 0.1 Ω cm, and increased with c_B [2]. The percolation threshold value was at about 50 wt %. At 70 and 90 wt % PTFE, ρ was 1 kΩ cm and 1 MΩ cm, respectively. The mechanical stability was reasonably high. The pellets endured a radial force of 2–4 N. The fabrication of a nanoporous 'monobloc' in the course of the pyrolysis step, without any binder [11, 20], seems not to be possible for CBs.

3.2. *CCC of single electrodes*

We employed constant current cycling (CCC, galvanostatic cycling) in a conventional three electrode glass cell as the experimental tool for the determination of the single electrode capacitance $C_{s,1}$. A typical result is shown in Figure 3. The potential–time curves exhibit arbitrarily linear behaviour, indicating nearly pure capacitances. The potential range was $U_s = -0.3$ to $+0.7$ V, corresponding to 0.37 to 1.37 V vs SHE. The slope of the linear parts, $v_S = dU/dt$, leads directly to the capacitance of the electrode:

$$C_1 = \frac{I}{v_S} \tag{2}$$

where I is the cycling current. $C_{s,1}$ is nearly constant from the beginning.

On the other hand, a carbon black with a very high specific area shows a remarkable initial decrease in C_s. The charge part of the CCC curves becomes flatter at high voltages, cf. Figure 4.

Figure 5 shows the result of an evaluation of the dependency of $C_{s,1}$ on the cycle number. Long term cycling of ECSC model cells, however, shows that a

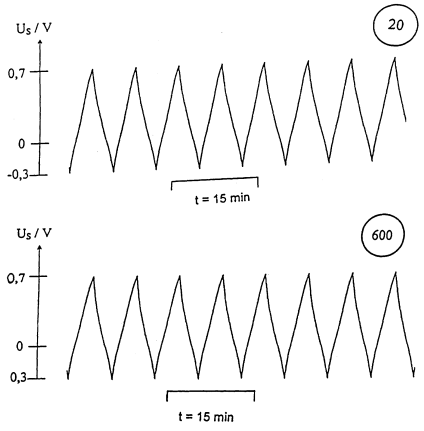

Fig. 3. Long term cycling (CCC) of single electrodes. CB: E 61 MM in 12 M H_2SO_4: $A_s = 1300$ m^2 g^{-1}, $C_{s,1} = 190$ F g^{-1}. Experimental conditions: $I = 100$ mA, $A = 4.54$ cm^2, $j = 22$ mA cm^{-2}, $U_s = -0.3$ to 0.7 V, m(CB) = 121 mg, m(PTFE) = 13.4 mg, Pt/Ti-holder (III). U_s means potential vs the Hg/Hg_2SO_4/1 M H_2SO_4 reference electrode, +674 mV vs SHE. Circled numbers indicate the cycle number.

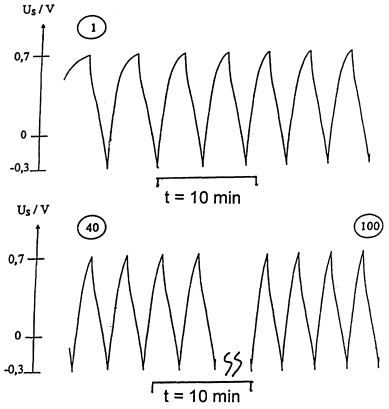

Fig. 4. Long term cycling (CCC) of single electrodes. CB: E 114 MM in 12 M H_2SO_4: Two independent runs. $A_s = 1690\ m^2\ g^{-1}$, $C_{s,1} = 250\ F\ g^{-1}$. Experimental conditions: $I = 156$ mA, $A = 4.54\ cm^2$, $j = 34\ mA\ cm^{-2}$, $U_s = -0.3$ to $+0.7$ V.

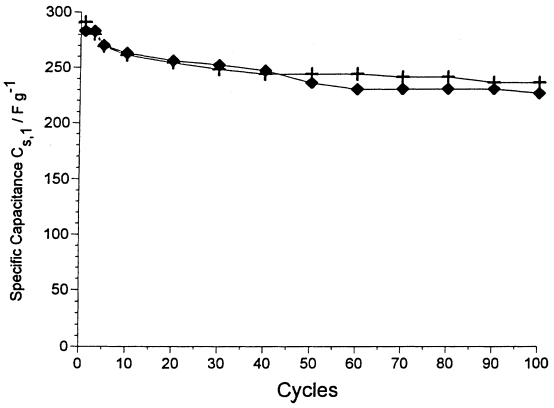

Fig. 5. Evaluation of Figure 4: Specific capacitance of the single electrode, $C_{s,1}$ in dependency on the cycle number.

steady state is established after about 150 cycles, cf. Figure 14.

An interesting behaviour within the first 10–20 cycles is exhibited by the carbon black electrodes. As shown in Figure 6, the charge Q_{ch} consumed during the charge period is appreciably larger than the charge Q_{disch} involved in the discharge period [2]. In other words, the charge factor $f = Q_{ch}/Q_{disch}$ is appreciably bigger than 1, $f > 1$. Accordingly, the current efficiency (c.e.) on cycling is initially $< 100\%$, but approaches nearly 100% after 20–30 cycles. A wholly analogous effect is reported for C-aerogel materials [11]. We agree with the interpretation given there: Unstable surface groups are irreversibly anodically oxidized. The cumulative total charge is roughly equivalent to the reversible capacitive charge.

3.3. *$C_{s,1}$ in dependency on A_s*

This dependency is a linear one on the basis of the Helmholtz double layer model, if the capacitance per atomic surface area, $C_{A,DL}$, is constant:

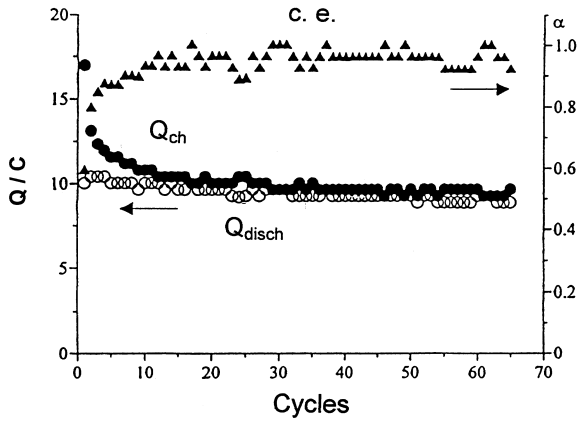

Fig. 6. Long term cycling (CCC) of a single electrode. Charges for the charge (Q_{ch}) and discharge (Q_{disch}) of a PCCB electrode. Current efficiencies (c.e.) are shown in addition. Experimental conditions: (CB) Black Pearls 2000 (Cabot), $A_s = 1475\ m^2\ g^{-1}$, 10 M H_2SO_4, $j = 34\ mA\ cm^{-2}$, $m = 39$ mg.

$$C_{s,1} = C_{A,DL} A_s \tag{3}$$

According to Figure 7 this relationship is confirmed by the experimental findings. The fit is much better for $C_{A,DL} = 16\ \mu F\ cm^{-2}$ than for $C_{A,DL} = 10\ \mu F\ cm^{-2}$. The former value follows from EIS measurements [2], while the latter is discussed in [4].

No.	ENSACO	A_s/m^2g^{-1}	C_s/F g^{-1}
1	E 61 MM	1300	200
2	ES 06 MM	1300	177
3	E 56 MM	1350	150
4	E 52 MM	1100	175
5	E114 MM	1690	265

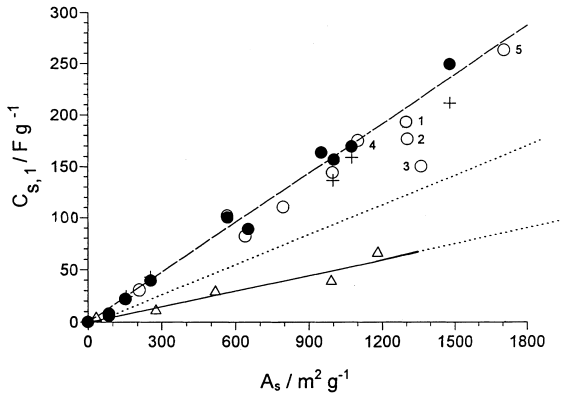

Fig. 7. Specific capacitance $C_{s,1}$ of precompacted (440 MPa) carbon black (CB) electrodes (10% PTFE as binder) vs specific surface A_s. A_s was obtained from BET measurements, $C_{s,1}$ from constant current cycling CCC at $j = 20$–$34\ mA\ cm^{-2}$ (cycle 10). (○) 12 M H_2SO_4 (CBs from MMM carbon), (●) 10 M H_2SO_4 (CBs from other manufacturers), +3 M H_2SO_4 (CBs from other manufacturers), (Δ) 1 M $LiCF_3SO_3$ in propylene carbonate. Key: (– – – –) calculated for a specific capacitance of the electrochemical double layer of $C_{A,DL} = 16\ \mu F\ cm^{-2}$, (·····) same, but $C_{A,DL} = 10\ \mu F\ cm^{-2}$.

Table 2. Calculation of $C_{s,1}$ after Equation 3 and comparison with the theoretical values

No.	$A_s/m^2\,g^{-1}$	Carbon black	$C_{A,DL}$ /$\mu F\,cm^{-2}$	$C_{s,1}$ /$F\,g^{-1}$ calc. after Equation 3	$C_{s,1}/F\,g^{-1}$ exp.
1	2629 (max)	(Theory)	16	420	–
2	2629 (max)	(Theory)	10	263	–
3	1690	E 114 MM	16	270	250
4	1690	E 114 MM	10	169	250
5	1475	Cabot Black Pearls 2000	16	236	240
6	1475	Cabot Black Pearls 2000	10	148	240
7	1300	E 61 MM	16	208	180
8	1300	E 61 MM	10	130	180

An analogous relationship was found for aprotic electrolytes [21], but the slope is only about 25%. This means that an aprotic ECSC with $U_{cell} = 2.0$–2.5 V would store the same specific energy E_s as an aqueous one with 1.0–1.2 V according to

$$E_s = \frac{1}{2} C_{s,cell} U_{cell}^2 \tag{4}$$

The CBs with a very high specific area are already close to the theoretical limit, which is given by the two-sided utilization of graphene layers [2]. This is summarized in Table 2. The experimental maximum of $C_{s,1} \approx 250\ F\,g^{-1}$ is about 60% of this theoretical upper limit. These findings agree with the purely capacitive behavior of CBs. The dashed line in Table 1 represents the limit where the specific area of the material can be calculated on the basis of compact (globular) particles according to

$$A_s = \frac{3}{r\rho} \tag{5}$$

where r is the radius of the particle, and ρ the density. For $r = 10$ nm and $\rho = 1\ g\,cm^{-3}$, Equation 5 gives $A_s = 300\ m^2\,g^{-1}$. As a consequence, higher A_s values lead to the assumption of nanopores in the particle. Unfortunately no direct (microscopic) evidence is available for the nanostructure of CB particles.

3.4. *Pseudo-capacitances*

The Helmholtz model of an atomic scale capacitor ($C_{A,DL} = 10$ to $20\ \mu F\,cm^{-2}$) represents a relatively low charge density at the surface. It is about 10% of that value, which would be obtained if every surface atom carried charge. The reason is, of course, lateral electrostatic repulsion. This limitation could be overcome by surface bound reversible redox systems, for example, of the quinone type:

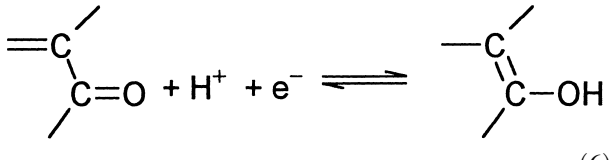

(6)

The redox states do not carry a free charge. Their molar surface concentration, Γ, may be appreciably higher. From this a pseudo capacitance $C_{A,P}$ follows:

$$C_{A,P} = \frac{d(zF\Gamma)}{d(\Delta\varphi)} \tag{7}$$

where $\Delta\varphi$ is the Galvani voltage. The capacitance of an ECSC would increase by one order of magnitude, as pointed out by Conway [22, 23]. We have studied the possible introduction of $C_{A,P}$ by anodic polarization [24]. An extension was indeed possible. Figure 8 gives an example [25].

The CV profile changes from a purely capacitive character to a cyclic curve with redox peaks. However, they are not reversible according to the usual criteria (peak separation). The chemical species must be located at the rim of the graphene layers. Graphite with extended graphene layers has only limited capabilities for the development of pseudo capacitances. Graphite intercalation compounds carry free electronic charges in the graphene layers, which are balanced by free ionic countercharges. Again, the charge density is about 10% of the theoretical maximum, but amorpheous carbons such as CBs, with a limited extension of the graphene layers (and a high portion of rims) are very suitable for the introduction of surface bound redox centres according to Equation 6.

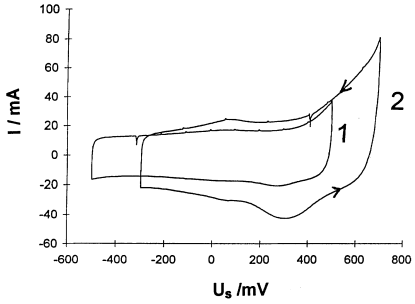

Fig. 8. In situ activation of E 61 MM by slow cyclic voltammetry, $v_S = 2\ mV\,s^{-1}$, 10th cycle. (1) $m = 71.8$ mg, potential range U_s = from −0.50 to +0.50 V, $C_{s,1} = 127\ F\,g^{-1}$; (2) $m = 76.7$ mg, potential range U_s = from −0.30 to +0.70 V, $C_{s,1} = 199\ F\,g^{-1}$.

3.5. *Current collectors and model cells for ECSCs*

Current collectors made from Pt are optimum due to their corrosion resistance in acid and their low wet contact resistance. However, their application in a practical ECSC is prohibitive due to costs and weight. We have developed CB filled polypropylene (RPP) as a possible low cost material [26]. Figure 9 compiles the results of a further development [27]. Resistivity ρ is about 1 Ω cm at a concentration level of $c_F = 30$ wt % CB. It comes down to 0.3–0.4 Ω cm, if c_F is raised to 40 wt %. But the composite may be very brittle, as it is the case for example (2). The foils represented by (1) are rather flexible, and this demonstrates clearly that the choice of the appropriate polymer binder is rather important. A huge amount of experience and know how for the fabrication of CB-filled polymers is present in the literature, cf. [28]. It should be mentioned that the ρ values, which were reported in [26] were higher than those in Figure 9. The reason for this is the electronic contact. In [26], a polished stainless steel plate was pressed onto the sample. But in Figure 9, a contact aid in terms of finely powdered graphite (Lonza T 15) was employed in addition.

Glassy carbon can be electrochemically activated to form an ECSC electrode [29, 30]. The process is lengthy. The basis material is rather expensive. The thickness ratio d(activated layer):d(GC_x = current collector) ≈ 1:10 is somewhat unfavourable. In the systems described in the present paper, the inverse ratio can be realized in principle. There are fundamental differences in the materials for current collectors, if aqueous or nonaqueous electrolytes are considered, cf. Table 3.

The general structure of an ECSC is laminated: current collectors (CC)|carbon(C)|Separator(S)|C|CC [31]. The optimum thicknesses are, with regard to the current collector, $d_{CC}:d_C:d_S = 1: > 1: \ll 1$. The separator was a thin ($d_S = 64$–114 μm), microporous polypropylene foil, Celgard™, from Celanese.

Figure 10 shows details of an experimental ECSC cell, which was employed for the measurements. The main part is a combination of two 'half elements', namely: (i) a current collector (base electrode) of Grafoil™ (UCC), Sigraflex™ (SGL Carbon) or RPP; (ii) a precompacted CB electrode (PCCBE), $A = 7$ cm^2; and (iii) a Celgard™ separator, which is glued to (i) at the rim. (i) and (iii) form a 'bag', with (ii) in the interior. Two such 'half elements' are combined according to Figure 10 to form a monopolar cell. In the corresponding bipolar design n such pairs are stacked. This means that two base electrodes form a bipolar wall which separates the bipolar units.

3.6. *Single electrode behaviour in ECSC cells*

The electrochemical behaviour of the single electrodes in an ECSC cell is not identical. On approaching the

Table 3. Current collector characteristics

Item	Aqueous electrolyte	Nonaqueous electrolyte	Spring elongation /cm	Spring constant /N mm^{-1}	Force /N
1. Electrolyte example	12 M H_2SO_4	1 M NEt_4BF_4 in PC	I 0.8	73.8	59 (MPR-1)
2. Material	CB-filled polyolefin (25–40 wt %)	Aluminium	II 0.9	4.0	3.6 (other)
3. Volume resistivity	1 Ω cm	10^{-6} Ω cm			
4. Contact/current lead	Flat (bipolar design)	Side on is possible			
5. Corrosion stability in 12 M H_2SO_4	Excellent	No stability			

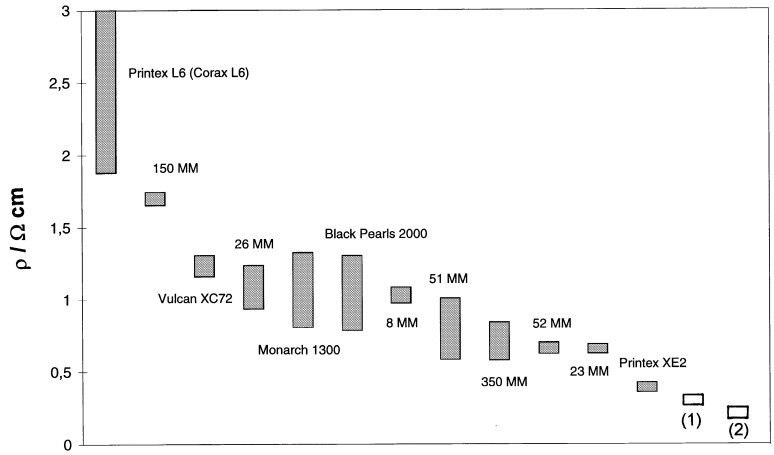

Fig. 9. Resistivities ρ of CB/PP composites 'RPP'. Dark rectangles: 30 wt % CB, as indicated, 1 mm plates, (PP) Novolen 1120 HX (BASF). Light rectangles: (1) 40 wt % Ensaco 350 MM Gran, Fina#-Binder; (2) 40 wt % Ensaco 350 MM Gran, DSM (19MN10)-binder.

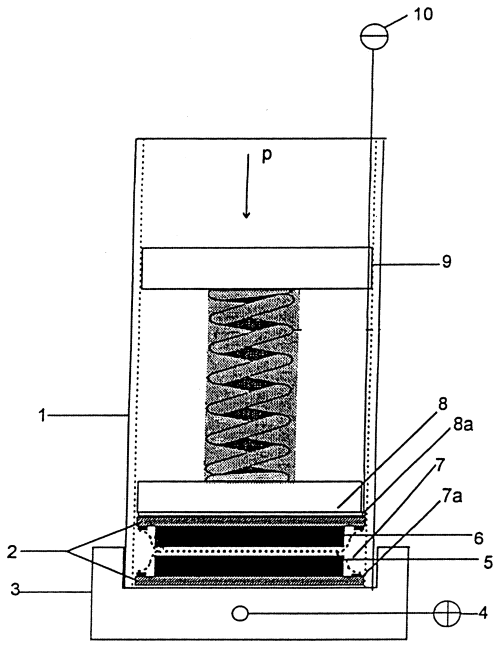

Fig. 10. ECSC model cell. A_{Pellet} = 7.1 cm^2, d_{Pellet} = 3 cm. Inner area of the cell: A_i = 20 cm^2. Separator: Celgard (porous PP, Celanese). Base electrode: Grafoil. 12 M H_2SO_4 as electrolyte. Key: (1) cylindrical cell, polypropylene, with an inner-threat, (2) Grafoil (graphite foil, UCC), (3) bottom of the cell, 18/8 stainless steel, (4) current lead, (5) positive CB electrode, (6) negative CB electrode, (7) Celgard-separator, (7a) glue line, (8) polypropylene-block, (8a) platinum-disc, (9) polypropylene disc with thread and (10) current lead.

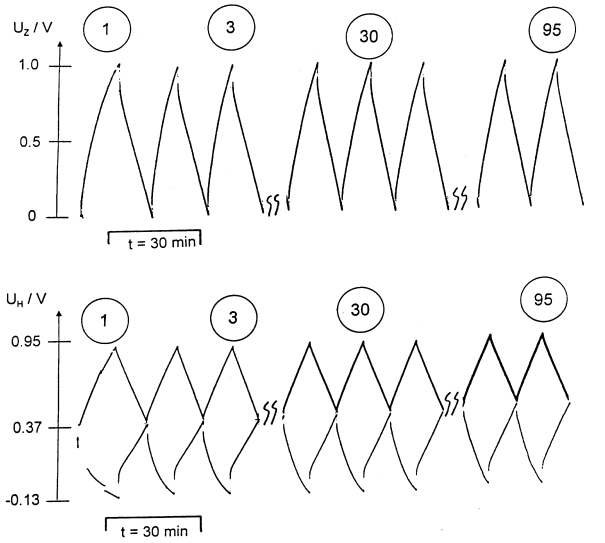

Fig. 11. CCC of a ECSC cell under simultaneous measurement of U_{cell} (U_Z), $U_{pos.}$ and $U_{neg.}$ vs SHE. Experimental conditions: CB: E114 MM, I = 100 mA, 12 M H_2SO_4, U_Z = 1 V, d = 3 cm, A = 7.07 cm^2, j = 14.15 mA cm^{-2}, m(Pel/pos) = 1.069 g, wt CB = 90%, m(Pel/neg) = 1.061 g, wt CB = 90%.

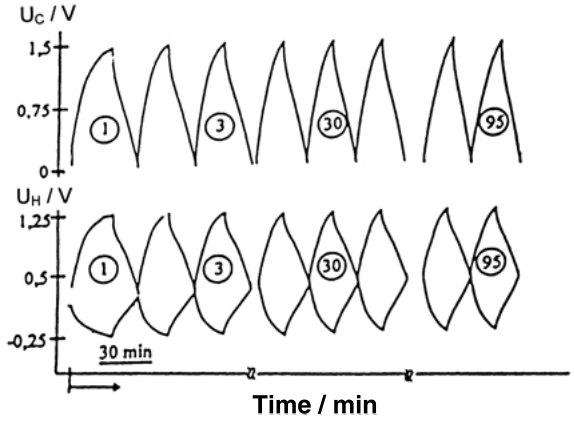

Fig. 12. CCC of a ECSC cell under simultaneous measurements of U_{cell} (U_Z), $U_{pos.}$ and $U_{neg.}$ vs SHE. Experimental conditions: CB: Black Pearls 2000, I = 100 mA, 10 M H_2SO_4, U_Z = 1.5 V, j = 14.15 mA cm^{-2}, m(Pel/pos) = 1.08 g, wt CB = 90%, m(Pel/neg) = 1.06 g, wt CB = 90%.

maximum voltage, the purely capacitive charge and discharge changes to that of a mixed electrode, with faradaic processes (e.g., hydrogen evolution at the negative). Possible interactions with the initial parts of the curves and even with the counter electrode are obvious. Figure 11 shows such a measurement in terms of single electrode potentials (vs SHE) and cell voltages at a cell voltage of 1.0 V. In this case, a rather 'ideal' capacitive behaviour is observed almost from the beginning. The negative shows an initial voltage drop due to the relatively high contact resistance.

Another measurement was performed at the higher end voltage of the cell, U_Z = 1.5 V [2]. In this case the single electrode behaviour varied widely. Even after 95 cycles no total coincidence could be attained. Especially the charge part deviated strongly from a pure capacitive behaviour. A greater part of the cell voltage was located at the positive.

3.7. *Long term cycling of ECSC cells*

An extremely high number Z of cycles can be expected if faradaic processes are absent. Such results are reported frequently. Figure 13 shows an example for the present system. An ECSC model cell according to Figure 10 was cycled at a constant current of 0.1 A. The run was finished after 2000 cycles, cf. Figure 13. A very even CCC behaviour was observed, with the exception of the very first cycles. The capacitance of the cell was evaluated with the aid of Equation 2 to be C_{cell} = 68 F at Z = 10 and 63 F at Z = 200, where a steady state was established. The initial loss in C_{cell} is analogous to the findings with single electrodes, cf. Section 3.2. This must be attributed to the formation of CB materials of very high specific area, as is the case for E114 MM. Figure 14 depicts the plot of C_{cell} against Z. The current efficiency, α, rapidly approaches 100%. The initial deviations to $\alpha < 1$ agree with those from single electrodes, cf. Figure 6. These results could be reproduced in three independent runs. The CB-mass in Figures 13 and 14 was 1.031 g at each electrode. The specific capacitance of the cell is therefore $C_{s,cell}$ = 33 (Z = 10) and

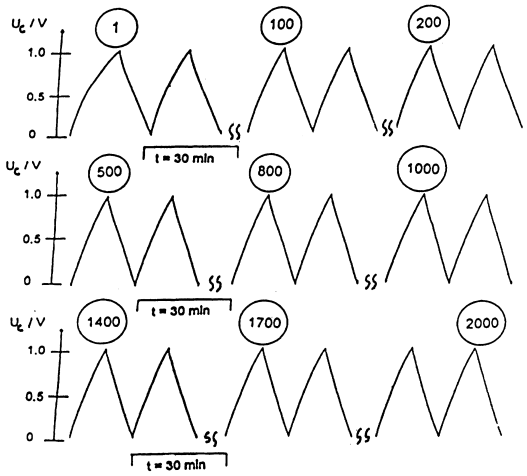

Fig. 13. Long term cycling of a ECSC model cell. Experimental conditions: CB: E114 MM, I = 100 mA, 12 M H_2SO_4, U_Z = 1 V, d = 3 cm, A = 7.07 cm^2, j = 14.15 mA cm^{-2}, m(CB/pos) = 1.0625 g, wt CB = 97%, m(CB/neg) = 1.0635 g, wt CB = 90%.

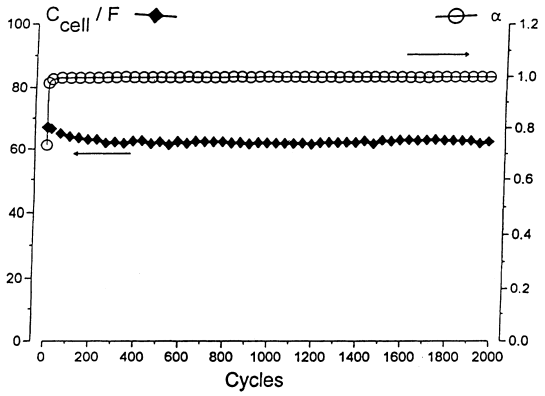

Fig. 14. Evaluation of Figure 13: specific capacitance of the cell, $C_{s,cell}$, in dependency on the cycle number.

30.5 F g^{-1} (Z = 200). From theory, the following relationship holds:

$$C_{s,1} = 4\ C_{s,cell} \tag{8}$$

The specific capacitance for single electrodes with the same C is given by $C_{s,1}$ = 230 F g^{-1} (after 100 cycles), cf. Sections 3.2 and 3.3 and Figure 5. Thus, our results for cells do not fulfill Equation 8. The reason for this is not clear.

A *bipolar cell* with five units switched in series was also successfully cycled. The capacitance decreased to 10 F instead of 60/5 = 12 F. The voltage increased to the theoretical value of U = 5 V. 700 cycles could be achieved. But thereafter a continuous decrease occurred within the next 100 cycles. This was due to a dry up effect.

Self discharge of cells or single electrodes was also studied. Conway has discussed several mechanisms [32]. Our results will be reported elsewhere [33].

4. Conclusions

Highly dispersed and/or highly porous carbon materials such as industrial carbon blacks (CBs) were investigated for development of ECSCs to be operated in a useful potential range (in 10–12 M H_2SO_4: U_H = 0.3 ... 1.5 V vs SHE). The results suggest that:

(i) The real surface of the CBs is utilized to a high degree. This is concluded from a proportionality of the specific capacitance C_s with specific area (BET) A_s.
(ii) For activated carbons this relationship is more complicated, due to the diversified structure of nanopores [8, 14].
(iii) With respect to the surface atoms of the material, only about 10% carry a free charge due to the electrostatic repulsion. This is comparable to the in plane order of graphite intercalation compounds.
(iv) An improvement should be possible through the introduction of pseudo capacitances. However, C-surfaces seem to have only a low surface concentration of the corresponding quinoide groups.
(v) RC-elements have to be identified at an atomic level in the future.

We propose a design of ECSCs, which is totally metal free [34, 35]. The following advantages can be stated: low cost industrial CB as active material; minimization of weight due to high C_s; no corrosion: carbon, graphite and polyolefins are absolutely stable in 10–12 M H_2SO_4; production technology is based on industrial polymers such as polypropylene; insulation capability of polypropylene; and easy manufacture of microporous materials (e.g. on the basis of polypropylene as separator).

Acknowledgements

Financial support through a BRITE/Euram Project 'ATES' (no. BRPR-CT 96-0233) is gratefully acknowledged. We are obliged to the companies which are quoted in Table 1, for the kind provision of carbon black samples and to C.H. Erbslöh, Krefeld, for the PTFE emulsion.

References

1. F. Krüger and F. Beck, *in* V. Barsukov and F. Beck (Eds), 'New Promising Electrochemical Systems for Rechargeable Batteries', (Kluwer Academic, Dordrecht, 1996), pp. 373–389.
2. F. Krüger, PhD thesis, Universität Duisburg (1997).
3. J.P. Donnet, R.C. Bansal and M.J. Wang (Eds), 'Carbon Black', 2nd edn (Marcel Dekker, New York, 1993).
4. K. Kinoshita, 'Carbon: Electrochemical and Physicochemical Properties' (J. Wiley & Sons, New York, 1988).
5. S. Sekido, T. Muranaka, Y. Yoshino and H. Mori, *Nation. Technic. Report* **26** (1980) 220.
6. Y. Kibi, T. Saito, M. Kurata, J. Tabuchi and A. Ochi, *J. Power Sources* **60** (1996) 219.
7. M.F. Rose, C. Johnson, T. Owens and B. Stephens, *J. Power. Sources* **47** (1994) 303.

8. H. Shi, *Electrochim. Acta* **41** (1996) 1633.
9. L. Bonnefoi, P. Simon, J.F. Fauvarque, C. Sarrazin, J.F. Sarrau and A. Dugast, *J. Power Sources* **80** (1999) 149.
10. M. Endo, Y. Okada and H. Nakamura, *Synthetic Metals* **34** (1989) 739.
11. S.T. Mayer, R.W. Pekala and J.L. Kaschmitter, *J. Electrochem. Soc.* **140** (1993) 446.
12. F. Beck, F. Krüger and H. Krohn, *GDCh-Monographie* **12** (1998) 331.
13. F. Beck, H. Krohn, F. Krüger and D. Kloss, Extended Abstracts 50th ISE Meeting in Pavia (Italy), 5–10. Sept. (1999), Vol. 1, No. 200.
14. D. Qu and H. Shi, *J. Power Sources* **74** (1998) 99.
15. I. Tanahashi, A. Yoshida and A. Nishino, *Bull. Chem. Soc. Japan* **63** (1990) 3611.
16. K.S.W. Sing, 'Adsorption, Surface Area and Porosity', 2nd edn (Academic Publishers, London, 1982).
17. F. Beck, *Electrochim. Acta* **17** (1972) 2317.
18. F. Beck and F. Krüger, *GDCh-Monograph.* **3** (1996) 465.
19. F. Beck and M. Dolata, *J. Electroanal. Chem.*, in press.
20. D.W. Firsich, *in* F.M. Delnick, D. Ingersoll, X. Andrieu and K. Naoi, 'Electrochemical Capacitors II', Proceedings Volume **96-25**, The Electrochemical Society, Pennington, NJ (1997), pp. 235–243.
21. M. Andrieu and L. Josset, Extended Abstracts, Electrochemical Society Meeting, Chicago, Oct. (1995), Abstract no. 57, p. 89.
22. B.E. Conway, *J. Electrochem. Soc.* **138** (1991) 1539.
23. B.E. Conway, V. Birss and J. Wojtowicz, *J. Power Sources* **66** (1997) 1.
24. F. Beck, F. Krüger and B. Wermeckes, *GDCh-Monographie* **9** (1997) 919.
25. R. Chromik, unpublished work (1999).
26. F. Beck, G. tom Suden, U. Tormin and T. Boinowitz, *Electrochim. Acta* **41** (1996) 933.
27. O. Niemzig, unpublished work (1997).
28. R. Gilg, *in* H.J. Mair and S. Roth (Eds), 'Elektrisch leitende Kunststoffe' (Carl Hanser Verlag, München, 1989).
29. D. Jürgen and E. Steckhan, *J. Electroanal. Chem.* **333** (1992) 177.
30. C. Barbero and R. Kötz, *J. Electrochem. Soc.* **140** (1993) 1.
31. E.T. Eisenmann, *Extended Abstracts*, Electrochemical Society Meeting, Chicago, Oct. (1995).
32. B.E. Conway, 'Electrochemical Supercapacitors' (Kluwer Academic/Plenum Publishers, New York, 1999), pp. 557–596.
33. F. Beck, R. Chromik and M. Dolata, *J. Power Sources*, in preparation.
34. F. Beck, *in* V. Barsukov and F. Beck (Eds), *loc. cit.* [1], pp. 393ff.
35. F. Beck: Graphite, carbonaceous materials and organic solids as active electrodes in metal-free batteries, *in* R.C. Alkire, H. Gerischer, D.M. Kolb and Ch. Tobias (Eds), '*Advances in Electrochemical Science and Engineering*' (VCH/Wiley, New York and Weinheim, 1997), pp. 303ff.